HOKKAIDO UNIVERSITY

Title	Differences in morphological features and minimum apparent diffusion coefficient values among breast cancer subtypes using 3-tesla MRI
Author(s)	Kato, Fumi; Kudo, Kohsuke; Yamashita, Hiroko et al.
Citation	European journal of radiology, 85(1), 96-102 https://doi.org/10.1016/j.ejrad.2015.10.018
Issue Date	2016-01
Doc URL	https://hdl.handle.net/2115/63971
Rights	© 2016. This manuscript version is made available under the CC-BY-NC-ND 4.0 license http://creativecommons.org/licenses/by-nc-nd/4.0/
Rights(URL)	https://creativecommons.org/licenses/by-nc-nd/4.0/
Type	journal article
File Information	manuscript.pdf

Hokkaido University Collection of Scholarly and Academic Papers : HUSCAP

Differences in morphological features and minimum apparent diffusion coefficient values among breast cancer subtypes using 3-tesla MRI

Fumi Kato MD, PhD[1)] fumikato@med.hokudai.ac.jp

Kohsuke Kudo MD, PhD[1)] kkudo@huhp.hokudai.ac.jp

Hiroko Yamashita MD, PhD[2)] hirokoy@huhp.hokudai.ac.jp

Jeff Wang[3)] jeff.wang@pop.med.hokudai.ac.jp

Mitsuchika Hosoda MD, PhD[2)] hosodam@seagreen.ocn.ne.jp

Kanako C Hatanaka MD, PhD[4)] kyanack@huhp.hokudai.ac.jp

Rie Mimura MD[1)] r_mimufam@huhp.hokudai.ac.jp

Noriko Oyama-Manabe MD, PhD[1)] norikooyama@med.hokudai.ac.jp

Hiroki Shirato MD, PhD[3)] shirato@med.hokudai.ac.jp

1) Department of Diagnostic and Interventional Radiology, Hokkaido University Hospital, N14, W5, Kita-ku, Sapporo, Japan, 060-8648

2) Department of Breast Surgery, Hokkaido University Hospital, N14, W5, Kita-ku, Sapporo, Japan, 060-8648

3) Department of Radiation Medicine, Hokkaido University Graduate School of Medicine, N15, W7, Kita-ku, Sapporo, Japan, 060- 8638

4) Department of Surgical Pathology, Hokkaido University Hospital, N14, W5, Kita-ku, Sapporo, Japan, 060-8648

Corresponding author: Kohsuke Kudo

E-mail: kkudo@huhp.hokudai.ac.jp

TEL: +81-11-706-5977, FAX: +81-11-706-7876

Abstract

Purpose: To compare the morphology and minimum apparent diffusion coefficient (ADC) values among breast cancer subtypes.

Methods: Ninety-three patients, who underwent breast MRI and collectively had 98 pathologically proven invasive carcinomas, were enrolled. Morphology was evaluated according to BIRADS-MRI. Minimum ADC was measured. Morphology and minimum ADC were compared among subtypes. Multivariate logistic regression analyses were used to identify the characteristics associated with different subtypes.

Results: Oval/round shape was significantly associated with triple-negative (TN) cancer (TN vs. non-TN: 90.9% vs. 45.2%; $p = 0.0123$). Rim enhancement was significantly less frequent in Luminal A (Luminal A vs. non-Luminal A: 34.2% vs. 76.1%; $p = 0.0003$). The minimum ADC of Luminal A was significantly higher than that of Luminal B (HER2-negative) (834 vs. 748 $\times 10^{-6}mm^2/s$; $p < 0.025$). The minimum ADC of the TN-special type was significantly higher than that of TN-ductal (997 vs. 702 $\times 10^{-6}mm^2/s$; $p < 0.025$). On the multivariate analysis comparing the characteristics associated with Luminal A versus Luminal B (HER2-negative), the internal enhancement characteristics of the mass and minimum ADC were significant factors.

Conclusion: Morphology and minimum ADC would be useful in distinguishing breast cancer subtypes**.**

Keyword

Breast cancer subtypes, Magnetic resonance imaging, Diffusion weighed imaging, Ki-67

Introduction

It has become generally accepted concept to regard breast cancer as a group of heterogeneous diseases rather than a single disease [1]. Using an immunohistochemical examination of the amounts of estrogen receptor (ER), progesterone receptor (PgR), human epidermal growth factor receptor 2 (HER2), and Ki-67 expression which reflects cellular proliferation, breast cancers are classified into several subtypes [1]. Breast cancer subtypes have different clinical features, including different prognoses and responses to therapies [1-5]. Therefore, non-invasive prediction of subtype using magnetic resonance imaging (MRI) is a desirable approach for selecting therapies.

Several reports have compared diffusion weighted imaging (DWI) and apparent diffusion coefficient (ADC) values in addition to the morphological characteristics on MRI with various pathological findings and biomarkers of breast cancer [6-11]. The ADC reflects the microenvironment of the tissue structures and is therefore related to the malignant features, such as cellularity, of the tumor. Most of the studies used mean ADC [6, 9]; however, the usefulness of minimum (min) ADC, which may reflect the most malignant portions of the tumor, in differentiating between malignant and benign breast masses and in detecting an invasive component in ductal carcinoma in situ has recently been reported [12, 13]. Additionally, ADC might reflect other characteristics of tissue structures, such as the amount of fibrous stroma and the

degree of cellular proliferation or nuclear atypia. Therefore, we hypothesized that the min ADC might be related to the breast cancer subtypes or biomarkers, too.

In addition to various subtypes, triple-negative (TN) breast cancer has heterogeneity; both invasive ductal carcinomas, which tend to exhibit low differentiation and poor prognosis, and special type breast cancers such as adenoid cystic carcinoma and medullary carcinoma, which tend to have relatively good prognosis, are included [1, 14]. Therefore, differentiation of these two subgroups, in addition to subtype, is also important. In addition to tumor cellularity, the ADC possibly reflects the microstructural characteristics—such as tubules, pseudocysts, and matrices—that can exist in several special types of cancers. Therefore, we considered that the min ADC might have the potential to distinguish between invasive ductal carcinomas and special types in TN breast cancers, reflecting their different histopathology.

The purposes of this study are (1) to compare morphological features and min ADC values among breast cancer subtypes, including TN cancer subgroups, and (2) to investigate the correlation between the Ki-67 index and min ADC in comparison with mean ADC values.

Materials and Methods

This retrospective study was approved by our institutional review board, and informed consent was waived. From February 2012 to June 2013, 95 consecutive patients who underwent breast MRI at 3-tesla (T) before operation without chemotherapy and hormonal therapy and had pathologically proven invasive carcinoma in operation specimens were studied. Two patients were excluded because of the difficulty in detecting the tumor on MRI; one had a small lesion with a large hematoma after biopsy in the breast, and another had marked background enhancement. Therefore, 93 patients were enrolled in this study. The median age was 60 years (range: 32-84 years), and all patients were women. The median interval between MR examination and operation was 29 days (range: 7-153).

There were 98 invasive carcinomas in 93 patients; three patients had bilateral breast carcinomas and two patients had two independent unilateral breast carcinomas. Independent unilateral cancers were considered when the pathological diagnosis or the ER, PgR, and HER2 receptor status of these cancers were different. The 98 lesions consisted of 80 invasive ductal carcinomas, 8 invasive lobular carcinomas, 2 invasive apocrine carcinomas, 2 tubular carcinomas, 2 metaplastic carcinomas, 1 adenocarcinoma, 1 invasive micropapillary carcinoma, 1 matrix-producing carcinoma, and 1 mucinous carcinoma.

Immunohistochemical (IHC) and Dual color in situ hybridization (DISH) analysis

Immunohistochemistry was performed for ER, PgR, HER2, and Ki-67 on serial 4-μm thick sections using the PATHWAY rabbit monoclonal antibodies (clones SP1, 1E2, and 4B5, respectively) and the iView DAB Detection Kit (Ventana Medical Systems, Inc., Tucson, AZ, USA). The expression of ER and PgR was estimated by staining the nuclei of cells and was considered positive when the percentage of positive cells was at least 1%. To determine the level of HER2 expression, the staining pattern of the membrane was estimated and scored on a scale of 0 to 3+. Tumors with a score of 2+ were tested for gene amplification by DISH (Ventana INFORM HER2 Dual ISH DNA Probe Cocktail; Roche Diagnostics, Tokyo, Japan). A ratio of HER2 gene to chromosome 17 > 2.2 was considered positive. Tumors were considered HER2-positive if IHC staining was 3+ or DISH positive. IHC for Ki67 was performed with mouse monoclonal anti-human Ki67 antibody (MIB-1, Dako, Glostrup, Denmark) at a 1:200 dilution. The Dako FLEX Envision system was used for visualization. The labeling index (LI) was assessed as the percentage of tumor cells, out of > 1000 invasive tumor cells, that showed definite nuclear staining using the NanoZoomer 2.0-HT (Hamamatsu photonics, Hamamatsu, Japan) for slide scanning and Tissue Studio (Definiens, Munich, Germany) for automated scoring.

The results of IHC and DISH analyses are as follows: ER-positive = 80, ER-negative

= 18, PgR-positive = 69, PgR-negative = 29, HER2-positive = 14, HER2-negative = 84, and the median of the Ki-67 index was 12.6% (range: 0.3–98.5).

With the ER, PgR, HER2 receptor status and cut-off of 14% with the Ki-67 index, the tumor subtypes were categorized as Luminal A, Luminal B (HER2-negative), Luminal B (HER2-positive), HER2-positive, and TN. TN breast cancers were further divided into the two subgroups of invasive ductal carcinoma (TN-ductal) and special type (TN-special) according to histological diagnosis. Of the 98 lesions, 46 were Luminal A, 25 were Luminal B (HER2-negative), 9 were Luminal B (HER2-positive), 5 were HER2-positive, 7 were TN-ductal, and 6 were TN-special. The TN-special lesions included 2 invasive apocrine carcinomas, 2 metaplastic carcinomas, 1 matrix-producing carcinoma, and 1 adenocarcinoma.

MRI technique

MR imaging was performed with a 3T system (Achieva TX; Phillips Medical Systems, Best, The Netherlands). A 7-channel breast coil was used, with the patient in the prone position.

Diffusion weighted images were acquired bilaterally in the axial plane with an echo planar imaging (EPI) sequence with fat suppression: TR/TE, 10,000 ms/52 ms; TI, 250 ms; FOV, 320 × 267 mm; voxel size, 3.33 × 4.18 × 5.00 mm; slice gap, 2 mm; NSA, 2; b values, 0 and 1000 s/mm^2; and SENSE factor: 2. STIR (short inversion-time inversion recovery) with SSGR

(slice selection gradient reversal) was used for fat suppression. The ADC values were calculated from two DWI scans acquired with b values of 0 and 1000 s/mm^2. The ADC maps were reconstructed by calculating the ADC values in each pixel of each section.

Dynamic contrast-enhanced images were acquired bilaterally in the axial plane with a 3-dimensional T1-weighted gradient echo sequence with fat suppression (e-Thrive): TR/TE, 4.9 ms/2.4 ms; flip angle, 10°; FOV, 320 × 320 mm; voxel size, 0.8 × 0.8 × 1.6 mm (reconstructed to 0.8 mm isovoxel), and SENSE factor, 2.4. Gadolinium-based contrast material at a dose of 0.1 mmol per kilogram of body weight was administered manually, followed by flushing with standardized 20-mL saline. Acquisitions before and three times (1, 2, and 6 minutes) after intravenous administration of contrast material were performed. High-resolution images were acquired during dynamic study (between 2 and 6 minutes) unilaterally on sagittal planes with 3-dimensional T1-weighted gradient echo sequences with fat suppression (e-Thrive): TR/TE, 4.5 ms/2.2 ms; flip angle, 10°; FOV, 150 × 150 mm; voxel size, 0.8 × 0.8 × 1.4 mm (reconstructed to 0.39 × 0.39 × 0.7 mm); and SENSE (-). High-resolution sagittal scans for the contralateral breast were obtained after dynamic scans, when needed.

Of 98 lesions, 44 (44.9%) were examined via MRI before biopsy and 54 (55.1%) were examined after biopsy.

Image analysis

Morphological evaluation

MR images were reviewed retrospectively by a board-certified radiologist specializing in breast MR imaging with 13 years of experience, without knowledge of the pathological findings other than invasive breast cancer. Both axial dynamic scans and sagittal high resolution scans were used for evaluation. For mass lesions, the shape, margin and internal enhancement characteristics were evaluated; and for non-mass lesions, the distribution and internal enhancement patterns were evaluated, based on the findings of Breast Imaging Reporting and Data System MRI [15].

ADC measurement

The ADC values of each lesion were measured by placing regions of interest (ROIs) within the targeted lesion on ADC maps. An oval-shaped ROI was placed inside the lesion, and made as large as possible while avoiding cystic or necrotic and hemorrhagic areas and obvious artifacts. When the lesion had both invasive and non-invasive components on the pathological specimen, ROI was placed on the suspected invasive component on MRI. The mean size of the ROIs was 68.9 mm^2 (range: 12.3-354.7). The min ADC values in each ROI were recorded, and the mean ADC values were also recorded for comparison.

Statistical Analysis

The tumor morphology on MRI was compared statistically among the subtypes using a χ^2 test. The min ADC values were compared statistically among the six subtypes using a non-parametric multiple comparison test (Kruskal-Wallis test with a post-hoc test). The correlation between the min and mean ADC values and Ki-67 indexes was investigated using Spearman's correlation coefficients. A receiver operating characteristic (ROC) curve was drawn to determine the best cut-off value of the min ADC value for discrimination between Luminal A and Luminal B (HER2-negative). Univariate and multivariate logistic regression analyses were used to identify the characteristics associated with different subtypes. The MedCalc 13.3.0.0 statistical software package (MedCalc Software bvba, Mariakerke, Belgium) was used for statistical analysis. All quantitative data are presented as the median and interquartile range. A p-value < 0.05 was considered significant.

Results

There were 84 (85.7%) masses and 14 (14.3%) non-mass enhancements on MRI. There was no significant difference in morphology (mass or non-mass) among subtypes (Table 1). In the 84 masses, there were significant differences in shape, margin, and internal enhancement characteristics among subtypes (Table 2), and in the 14 non-mass lesions, there were no significant differences among subtypes (Table 3). Oval/round shape was significantly associated with TN breast cancer (90.9% (10/11) in TN vs. 45.2% (33/73) in non-TN, p = 0.0123). Spiculated margins were significantly associated with ER-positive breast cancer (48.5% (33/68) in ER-positive vs. 6.3% (1/16) in ER-negative, p = 0.0048), especially Luminal A (Table 2). Rim enhancement was significantly less often seen in Luminal A than the other subtypes (34.2% (13/38) in Luminal A vs. 76.1% (35/46) in other subtypes, p = 0.0003).

Min ADC values were 834 (705, 1048) × $10^{-6}mm^2/s$ in Luminal A, 748 (678, 825) × $10^{-6}mm^2/s$ in Luminal B (HER2-negative), 763 (714, 882) × $10^{-6}mm^2/s$ in Luminal B (HER2-positive), 827 (727, 838) × $10^{-6}mm^2/s$ in HER2-positive, 702 (637, 752) x $10^{-6}mm^2/s$ in TN-ductal, and 997 (974, 1095) × $10^{-6}mm^2/s$ in TN-special, respectively (Figure 1), and the Kruskal-Wallis test showed significant (p = 0.013161). There was a large overlap in the min ADC values between most of the subtypes; however, the post-hoc test revealed that the min ADC value of Luminal A was significantly higher than that of Luminal B (HER2-negative) (p <

0.025) and TN-ductal ($p < 0.05$) (Figure 1), and min ADC value of TN-special was significantly higher than that of TN-ductal ($p < 0.025$), Luminal B (HER2-negative) ($p < 0.025$), and HER2-positive ($p < 0.05$) (Figure 1).

In the analysis of correlation between min and mean ADC and Ki-67, one lesion of Luminal B (HER2-positive) was excluded due to lack of Ki-67 measurement. A weak, but statistically significant correlation was observed between min ADC values and Ki-67 indexes ($r_s = -0.297$, $p = 0.0032$). The correlation between mean ADC values and Ki-67 indexes was also statistically significant ($r_s = -0.261$, $p = 0.0099$), but this correlation was weaker than that of min ADC. In the subgroup analysis, the Luminal (HER2-negative) subgroup, including Luminal A and Luminal B (HER2-negative) had a weak, but statistically significant correlation between min ADC values and Ki-67 ($r_s = -0.382$, $p = 0.001$). There were no significant correlations in the other subtypes ($p = 0.779$ ($n = 8$) in Luminal B (HER2-positive), $p = 0.285$ ($n = 5$) in HER2-positive, $p = 0.215$ ($n = 7$) in TN-ductal, and $p = 0.425$ ($n = 6$) in TN-special). The ROC curve analysis showed that the best cut-off value of min ADC for the discrimination of Luminal A from Luminal B (HER2-negative) was $904.276 \times 10^{-6} mm^2/s$ with 34.8% sensitivity and 96.0% specificity (AUC = 0.672, $p = 0.007$).

Table 4 shows the results of univariate and multivariate analyses comparing the characteristics associated with Luminal A versus Luminal B (HER2-negative). On univariate

analysis, the internal enhancement characteristics of the mass and min ADC were significant factors. In the multivariate model, both factors remained significant. The AUC of this model was 0.746.

Representative cases of Luminal A compared with Luminal B (HER2-negative) and TNs are shown in Figure 2 and 3, respectively.

Discussion

The present study demonstrated that there were differences in min ADC as well as morphological characteristics among breast cancer subtypes. Luminal A breast cancer tended to show a spiculated margin without rim enhancement and had significantly higher min ADC values than Luminal B (HER2-negative). TN breast cancer tended to show an oval/round shape with rim enhancement and exhibited significant differences in min ADC value between TN-ductal and TN-special. There were no significant findings for HER2-positive breast cancer.

A spiculated margin has been reported to be associated with low histological grade and low expression of Ki-67 (< 20%), while rim enhancement is associated with high histological grade and negative expression of ER and PgR [8]. Our results showing that Luminal A breast cancer tended to have a spiculated mass margin without rim enhancement were consistent with those previous reports. We also found that a spiculated margin was rarely seen in ER-negative cancers, indicating that a spiculated margin would be a major finding for distinguishing between ER-positive and ER-negative cancers.

Previous studies have reported that there was no significant correlation between ADC and Ki-67 [10, 11]. In our study, a weak but statistically significant correlation was observed between min ADC and Ki-67, especially in the Luminal (HER2-negative) subgroup. A correlation between ADC values and Ki-67 indexes was statistically significant both for min and

mean ADC; however, the correlation was better in min ADC than mean ADC. Most of the previous studies used mean ADC, which is the conventional method, but we demonstrated that min ADC had a better result in the correlation with Ki-67. Min ADC of Luminal A was significantly higher than that of Luminal B (HER2-negative), which reflects the difference of Ki-67 expression between Luminal A and Luminal B (HER2-negative). Therefore, a higher min ADC indicated Luminal A. According to our ROC analysis, Luminal A cancer could be distinguished from Luminal B (HER2 negative) with high specificity (96%).

In our multivariate analysis, internal enhancement characteristic of the mass and min ADC were significant in distinguishing Luminal A from Luminal B (HER2-negative). The AUC (0.746) of this model was higher than that (0.672) from the ROC analysis using the min ADC only. Combining the morphological and min ADC data could be more useful regarding predicting Luminal A.

It has been reported that TN breast cancers tend to have a round/oval mass shape [6] and have rim enhancement [6, 7]. Thus our results showing that TN breast cancers showed round/oval mass shape significantly more often than the other subtypes and had rim enhancement were consistent with those previous reports. In the present study, we divided TN cancers into two subgroups, TN-ductal and TN-special, because of the clinico-pathologic heterogeneity in TN cancers. There was no difference in morphological features between TN-ductal and TN-special;

most TN masses showed oval/round shape (100% in TN- ductal and 80% in TN-special), none of the TN-ductal or TN-special masses exhibited a spiculated margin, and most TN masses showed rim enhancement (83.3% in TN-ductal and 80% in TN-special) (Table 2). However, there was a significant difference in the min ADC value between them: the min ADC of TN-ductal was significantly lower than that of TN-special. Therefore the min ADC value could be used to distinguish between the ductal and special type of TN cancers. According to Youk et al., the ADC value of TN breast cancers (including both TN-ductal and TN-special) was higher than those for ER-positive and HER2-positive breast cancers [6]. In contrast, only TN-special cancer had a significantly higher min ADC than HER2-positive cancers in our study. If the heterogeneity of TN cancers is not considered and both TN-ductal and TN-special are treated as one group of TN cancers as in the previous report, the ADC value would change depending on the incidence of TN-ductal and TN-special in the study population.

In our study, TN-ductal had the lowest min ADC value among all subtypes. Because TN-ductal breast cancers are aggressive tumors with poor prognosis [16], our result reflects the malignancy of TN-ductal cancers. According to Basu et al., in TN breast cancers significantly higher fluorine-18 fluorodeoxyglucose (FDG) uptake was observed compared with the uptake in the ER-positive (HER2 negative) tumors on FDG-PET imaging, which is commensurate with their aggressive biology [17]. Our results were consistent with those of the previous FDG-PET

study.

It has been reported in previous studies that min ADC is useful for differentiating between malignant and benign breast masses or for detecting an invasive component in ductal carcinoma in situ [12, 13]. In the present study, we used the min ADC value to differentiate among breast cancer subtypes, and showed significant differences in several subtypes. However, there is a slight difference in the definition of min ADC between the above-mentioned previous studies on breast MRI and our own study; in the previous studies the min ADC was the lowest mean ADC value among multiple small ROIs placed within the targeted lesion [12, 13], whereas in our study the min ADC was the lowest value in the single ROI within the targeted lesion. The definition of our min ADC is commonly used [18-20]. The single ROI method might be more affected by outliers than the multiple ROI method; however, the single ROI method is feasible in clinical settings. When the ROIs were placed, we avoided cystic, necrotic, and hemorrhagic areas, as well as visual artifacts—which are possible causes of outliers—within the lesion.

In our study, more than half of the cancers were examined via MRI after biopsy. According to Latifoltojar et al., the ADC values of the prostate at 1, 2, and 6 months post biopsy were not significantly different from the pre-biopsy values [21]. Therefore, we assumed that biopsy did not have a very significant effect on ADC measurement. In addition, we avoided placing ROI in hemorrhagic areas.

There are several limitations to the present study. First, the study was retrospective and carried all the inherent limitations of retrospective investigations. Further prospective studies are needed to evaluate diagnostic performances of min ADC for differentiating tumor subtypes. Second, patients with chemotherapy or hormonal therapy before operation were not included in the present study. Therefore the numbers of TN and HER2-positive tumors were small, because patients with TN and HER2-positive tumors tend to receive neo-adjuvant chemotherapy. Third, for each tumor, we placed the ROI to measure the min ADC value on only one slice. We might have missed the most malignant portion in our single slice ROI measurement. If we had measured all the slices to find out the actual min ADC throughout the tumor, the results might be better. Fourth, the measurement positions between the min ADC value on MRI and the Ki-67 index in pathological specimens were different. We investigated the correlation between the ADC value and the Ki-67 index. The correlation should ideally be analyzed in the same position; however, it is difficult to completely match the position on MR images and pathological specimens in a factual manner.

Conclusion

Morphological features on 3T MRI would be helpful to distinguish breast cancer subtypes, especially in Luminal A and TN, a finding consistent with previous studies. There were significant differences between the min ADC values of Luminal A and Luminal B (HER2-negative) and between those of TN-ductal and TN-special. Min ADC values partially reflect the Ki-67 index, especially in Luminal (HER2-negative) breast cancers.

References

[1] Goldhirsch A, Wood WC, Coates AS, Gelber RD, Thurlimann B, Senn HJ. Strategies for subtypes--dealing with the diversity of breast cancer: highlights of the St. Gallen International Expert Consensus on the Primary Therapy of Early Breast Cancer 2011. Ann Oncol 2011;22(8):1736-47.

[2] Phipps AI, Buist DS, Malone KE, et al. Reproductive history and risk of three breast cancer subtypes defined by three biomarkers. Cancer Causes Control 2011;22(3):399-405.

[3] Liedtke C, Mazouni C, Hess KR, et al. Response to neoadjuvant therapy and long-term survival in patients with triple-negative breast cancer. J Clin Oncol 2008;26(8):1275-81.

[4] Dignam JJ, Dukic V, Anderson SJ, Mamounas EP, Wickerham DL, Wolmark N. Hazard of recurrence and adjuvant treatment effects over time in lymph node-negative breast cancer. Breast Cancer Res Treat 2009;116(3):595-602.

[5] Aebi S, Sun Z, Braun D, et al. Differential efficacy of three cycles of CMF followed by tamoxifen in patients with ER-positive and ER-negative tumors: long-term follow up on IBCSG Trial IX. Ann Oncol 2011;22(9):1981-7.

[6] Youk JH, Son EJ, Chung J, Kim JA, Kim EK. Triple-negative invasive breast cancer on dynamic contrast-enhanced and diffusion-weighted MR imaging: comparison with other breast cancer subtypes. Eur Radiol 2012;22(8):1724-34.

[7] Uematsu T, Kasami M, Yuen S. Triple-negative breast cancer: correlation between MR imaging and pathologic findings. Radiology 2009;250(3):638-47.

[8] Lee SH, Cho N, Kim SJ, et al. Correlation between high resolution dynamic MR features and prognostic factors in breast cancer. Korean J Radiol 2008;9(1):10-8.

[9] Razek AA, Gaballa G, Denewer A, Nada N. Invasive ductal carcinoma: correlation of apparent diffusion coefficient value with pathological prognostic factors. NMR Biomed 2010;23(6):619-23.

[10] Martincich L, Deantoni V, Bertotto I, et al. Correlations between diffusion-weighted imaging and breast cancer biomarkers. Eur Radiol 2012;22(7):1519-28.

[11] Kim SH, Cha ES, Kim HS, et al. Diffusion-weighted imaging of breast cancer: correlation of the apparent diffusion coefficient value with prognostic factors. J Magn Reson Imaging 2009;30(3):615-20.

[12] Hirano M, Satake H, Ishigaki S, Ikeda M, Kawai H, Naganawa S. Diffusion-weighted imaging of breast masses: comparison of diagnostic performance using various apparent diffusion coefficient parameters. AJR Am J Roentgenol 2012;198(3):717-22.

[13] Mori N, Ota H, Mugikura S, et al. Detection of invasive components in cases of breast ductal carcinoma in situ on biopsy by using apparent diffusion coefficient MR parameters. Eur Radiol 2013;23(10):2705-12.

[14] Leidy J, Khan A, Kandil D. Basal-like breast cancer: update on clinicopathologic, immunohistochemical, and molecular features. Arch Pathol Lab Med 2014;138(1):37-43.

[15] Breast imaging reporting and data system (BI-RADS) 5th edition. American College of Radiology, Reston, 2013.

[16] de Ruijter TC, Veeck J, de Hoon JP, van Engeland M, Tjan-Heijnen VC. Characteristics of triple-negative breast cancer. J Cancer Res Clin Oncol 2011;137(2):183-92.

[17] Basu S, Chen W, Tchou J, et al. Comparison of triple-negative and estrogen receptor-positive/progesterone receptor-positive/HER2-negative breast carcinoma using quantitative fluorine-18 fluorodeoxyglucose/positron emission tomography imaging parameters: a potentially useful method for disease characterization. Cancer 2008;112(5):995-1000.

[18] Inoue C, Fujii S, Kaneda S, et al. Apparent diffusion coefficient (ADC) measurement in endometrial carcinoma: effect of region of interest methods on ADC values. J Magn Reson Imaging 2014;40(1):157-61.

[19] Hida T, Nishie A, Asayama Y, et al. Apparent diffusion coefficient characteristics of various adrenal tumors. Magn Reson Med Sci 2014;13(3):183-9.

[20] Baba S, Isoda T, Maruoka Y, et al. Diagnostic and prognostic value of pretreatment SUV in 18F-FDG/PET in breast cancer: comparison with apparent diffusion coefficient from diffusion-weighted MR imaging. J Nucl Med 2014;55(5):736-42.

[21] Latifoltojar A, Dikaios N, Ridout A, et al. Evolution of multi-parametric MRI quantitative parameters following transrectal ultrasound-guided biopsy of the prostate. Prostate cancer and prostatic diseases 2015. http://dx.doi.org/10.1038/pcan.2015.33 [Epub ahead of print].

Figure legends

Figure 1: Minimum (min) apparent diffusion coefficient (ADC) values of each subtype.

The Kruskal-Wallis test showed significant ($p = 0.013161$). The min ADC value of Luminal A was higher than those of most of other subtypes, and statistically significant differences were noted for Luminal B (human epidermal growth factor receptor 2 (HER2)-negative) and triple negative (TN)-invasive ductal carcinoma (ductal) using the post-hoc test. The min ADC of TN-special type carcinoma (special) was also higher than those of the other subtypes, and the differences were significant for Luminal B (HER2-negative), HER2-positive, and TN-ductal using the post-hoc test.

*[1]-: -negative; *[2]+: -positive; *[3]TN: triple-negative.

Figure 2: A representative case of Luminal A breast cancer (a1-a4) compared with Luminal B (human epidermal growth factor receptor 2 (HER2)-negative) breast cancer (b1-b4). Sagittal contrast-enhanced fat-suppressed T1-weighed high-resolution imagings (a1, b1), axial dynamic contrast-enhanced fat-suppressed T1-weighed imagings 60 seconds after administration of gadolinium (a2, b2), axial diffusion-weighted imagings (DWI) with a b-value of 1000 s/mm^2 (a3, b3), and apparent diffusion coefficient (ADC) maps (a4, b4) are shown.

a: A 53-year-old woman with Luminal A breast cancer (tubular carcinoma; estrogen receptor

(ER): positive; progesterone receptor (PgR): positive; HER2: negative; Ki-67: 1.3%). A mass (shape: irregular; margin: irregular; and internal enhancement: heterogenous) is seen in the left breast (a1: circle; a2: arrow). On DWI the mass shows hyperintensity (a3: arrow). The ADC values of the mass are lower than the surrounding breast tissue (a4: arrow). The minimum (min) ADC of this lesion was $1062 \times 10^{-6} mm^2/s$.

b: A 52-year-old woman with Luminal B (HER2-negative) breast cancer (invasive ductal carcinoma; ER: positive; PgR: positive; HER2: negative; Ki-67: 17%). A mass (shape: irregular; margin: spiculated; and internal enhancement: heterogenous) is seen in the left breast (b1, b2: arrowhead). On DWI, the mass shows hyperintensity (b3: arrowhead). On the ADC map the mass was identified as a low value area compared to surrounding breast tissue (b4: arrowhead), and the values were lower than for Luminal A (a4). The min ADC of this lesion was $647 \times 10^{-6} mm^2/s$.

Figure 3: A representative case of triple-negative (TN) breast cancers (TN-invasive ductal carcinoma (ductal): a1-a4; TN-special type carcinoma (special): b1-b4). Sagittal contrast-enhanced fat-suppressed T1-weighed high-resolution imagings (a1, b1), axial dynamic contrast-enhanced fat-suppressed T1-weighed imagings 60 seconds after administration of gadolinium (a2, b2), axial diffusion weighted imagings (DWI) with a b-value of 1000 s/mm^2 (a3,

b3), and apparent diffusion coefficient (ADC) maps (a4, b4) are shown.

a: A 68-year-old woman with TN-ductal breast cancer (invasive ductal carcinoma; estrogen receptor (ER): negative; progesterone receptor (PgR): negative; human epidermal growth factor receptor 2 (HER2): negative; Ki-67: 38.8%). A mass (shape: oval; margin: irregular; and internal enhancement: rim enhancement) is seen in the left breast (a1, a2: arrow). On DWI the mass shows hyperintensity (a3: arrow). The ADC values are lower compared to surrounding breast tissue (a4: arrow). The minimum (min) ADC of this lesion was $545 \times 10^{-6} mm^2/s$.

b: A 68-year-old woman with TN-special breast cancer (invasive apocrine carcinoma; ER: negative; PgR: negative; HER2: negative; Ki-67: 10.8%). A mass (shape: oval; margin: irregular; and internal enhancement: rim enhancement) is seen in the right breast (b1, b2: arrowhead). Non-mass enhancements representing ductal carcinoma in situ are also seen (b1: arrows). On DWI the mass shows moderate hyperintensity (b3: arrowhead). On the ADC map the mass was identified as a slightly low value area compared to surrounding breast tissue (b4: arrowhead); however, the ADC values were higher than those for TN-ductal cancer (a4). The min ADC of this lesion was $998 \times 10^{-6} mm^2/s$.

Figure 1

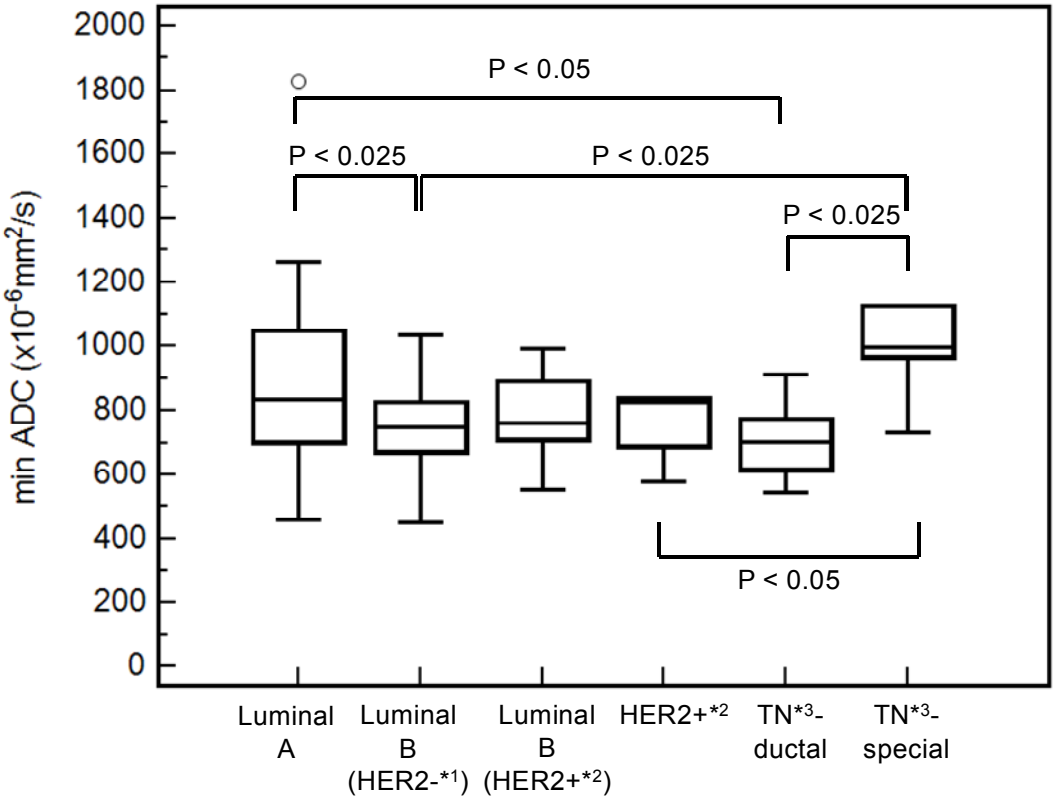

min ADC (x10-6mm2/s)
2000
1800
1600
1400
1200
1000
800
600
400
200
0
P < 0.05
P < 0.025
P < 0.025
P < 0.025
P < 0.05
Luminal A
Luminal B (HER2-*1)
Luminal B (HER2+*2)
HER2+*2
TN*3-ductal
TN*3-special

Figure 2

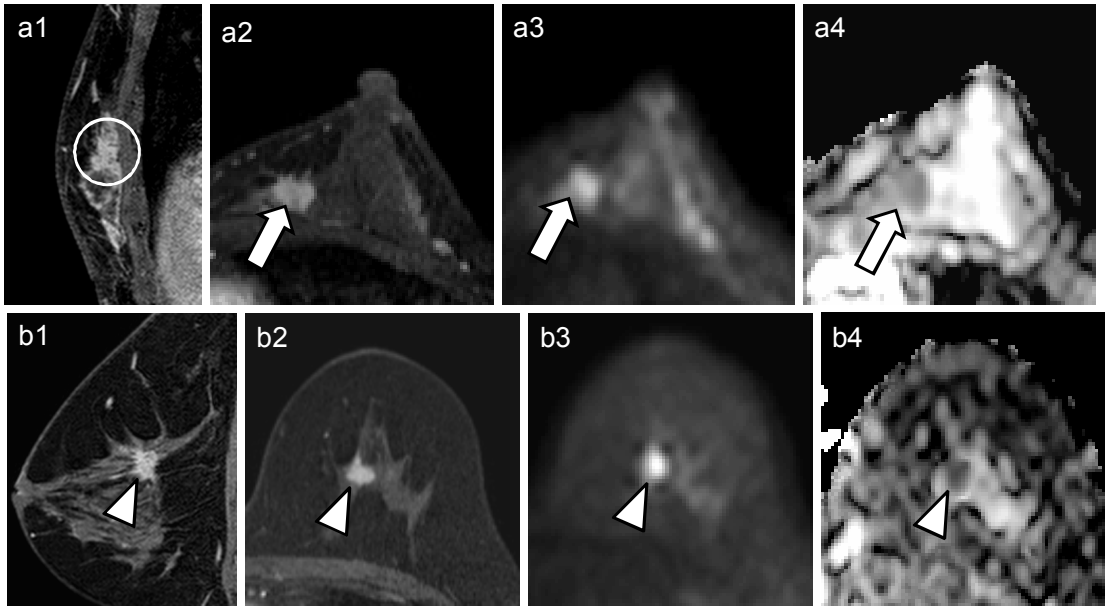


Figure 3

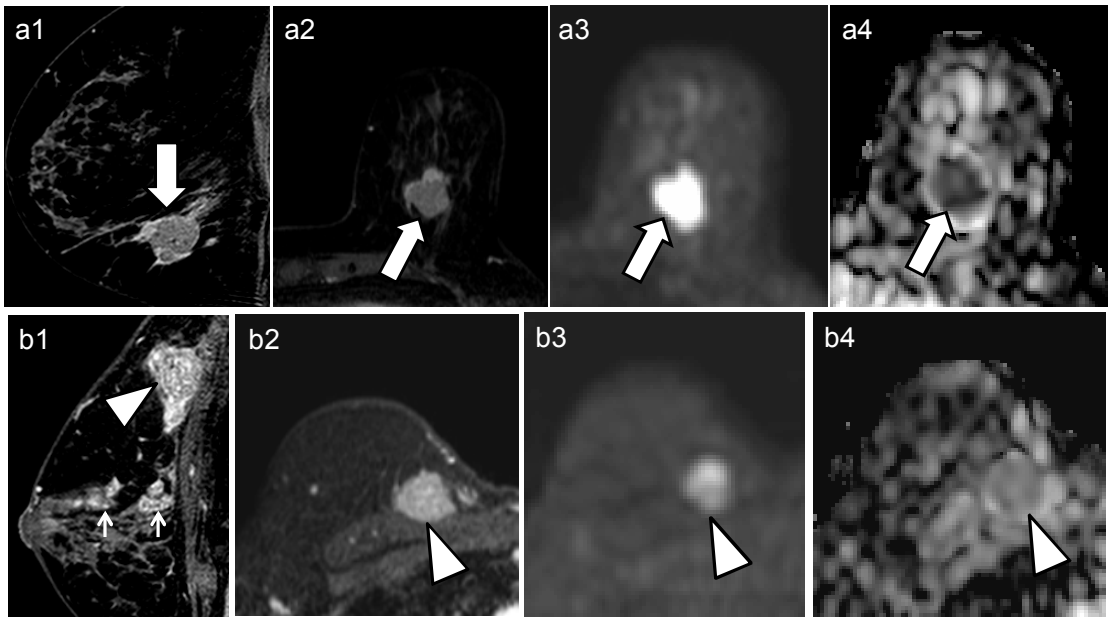


Table 1: Morphology in each subtype

	Luminal A	Luminal B (HER2-negative)	Luminal B (HER2-positive)	HER2-positive	TN-ductal	TN-special	P value
Mass	38	23	7	5	6	5	0.7775
Non-mass	8	2	2	0	1	1	

HER2 human epidermal growth factor receptor 2, *TN* triple-negative

Table 2: MR image findings of masses in each subtype

	Luminal A	Luminl B (HER2-negative)	Luminal B (HER2-positive)	HER2-positive	TN-ductal	TN-special	P value
Shape							
Oval / round	16	11	5	1	6	4	**0.0371**
Irregular	22	12	2	4	0	1	
Margin							
Irregular	16	14	5	4	6	5	**0.0186**
Spiculated	22	9	2	1	0	0	
Internal enhancement characteristics							
Heterogeneous	25	8	1	0	1	1	**0.0350**
Rim enhancement	13	15	6	5	5	4	

HER2 human epidermal growth factor receptor 2, *TN* triple-negative

Table 3: MR image findings of non-mass enhancement in each subtype

	Luminal A	Luminal B (HER2-negative)	Luminal B (HER2-positive)	HER2-positive	TN-ductal	TN-special	P value
Distribution							
Focal	3	1	0	0	0	0	0.9569
Linear	1	0	0	0	0	0	
Segmental	3	1	2	0	1	1	
Diffuse	1	0	0	0	0	0	
Internal enhancement patterns							
Heterogeneous	1	1	0	0	0	0	0.5845
Clumped	3	1	0	0	0	0	
Clustered ring	4	0	2	0	1	1	

HER2 human epidermal growth factor receptor 2, *TN* triple-negative

Table 4: Logistic regression analysis of factors associated with Luminal A versus Luminal B (HER2-negative)

	Univariate analysis		**Multivariate analysis**	
Variables analyzed	Odds ratio (95% CI)	P value	Odds ratio (95% CI)	P value
Shape				
Oval / round	1			
Irregular	1.2604 (0.445-3.5703)	0.6631		
Margin				
Irregular	1			
Spiculated	2.1389 (0.7437-6.1514)	0.1584		
Internal enhancement characteristics				
Heterogenous	1		1	
Rim enhancement	0.2773 (0.0934-0.8239)	**0.0210**	0.2392 (0.0737-0.7756)	**0.0172**
Min ADC	1.0036 (1.0006-1.0067)	**0.0184**	1.0045 (1.0006-1.0085)	**0.0252**

HER2 human epidermal growth factor receptor 2, *Min* minimum, *ADC* apparent diffusion coefficient